Contract No:

This document was prepared in conjunction with work accomplished under Contract No. DE-AC09-08SR22470 with the U.S. Department of Energy (DOE) Office of Environmental Management (EM).

Disclaimer:

SRNL-STI-2015-00031
Proceedings of the ASME 2015 Pressure Vessels & Piping Division Conference
PVP2015
July 19-23, 2015, Boston, Massachusetts, USA

PVP2015-45239

ANALYSIS OF PRESSURIZATION OF PLUTONIUM OXIDE STORAGE VIALS DURING A POSTULATED FIRE

James E. Laurinat
Savannah River National Laboratory
Savannah River Site, Aiken, SC 29808
Email: james.laurinat@srnl.doe.gov

Matthew R. Kesterson
Savannah River National Laboratory
Savannah River Site, Aiken, SC 29808
Email: matthew.kesterson@srnl.doe.gov

Steve J. Hensel
Savannah River Nuclear Solutions LLC
Savannah River Site, Aiken, SC 29808
Email: steve.hensel@srnl.doe.gov

ABSTRACT

The documented safety analysis for the Savannah River Site evaluates the consequences of a postulated 1000 °C fire in a glovebox. The radiological dose consequences for a pressurized release of plutonium oxide powder during such a fire depend on the maximum pressure that is attained inside the oxide storage vial. To enable evaluation of the dose consequences, pressure transients and venting flow rates have been calculated for exposure of the storage vial to the fire. A standard B vial with a capacity of approximately 8 cc was selected for analysis. The analysis compares the pressurization rate from heating and evaporation of moisture adsorbed onto the plutonium oxide contents of the vial with the pressure loss due to venting of gas through the threaded connection between the vial cap and body. Tabulated results from the analysis include maximum pressures, maximum venting velocities, and cumulative vial volumes vented during the first 10 minutes of the fire transient. Results are obtained for various amounts of oxide in the vial, various amounts of adsorbed moisture, different vial orientations, and different surface fire exposures.

INTRODUCTION

The Savannah River Site safety basis utilizes a graded approach to evaluate the radiological dose consequences of a pressurized release of plutonium dioxide powder during a postulated fire in a glovebox. The consequences depend on the maximum venting pressure and the amount of powder that is released. To provide input for the dose consequence evaluation, pressure transients and venting rates are analyzed for the exposure of a standard cylindrical oxide storage vial called a B vial to a 1000 °C fire. During the fire the vial pressurizes due to heating and evaporation of moisture adsorbed onto the oxide powder that it contains. Venting occurs through a threaded connection between the vial cap and body. The threaded connection sometimes is sealed by an o-ring, which would fail during the early stages of the fire. If the o-ring is absent, the top surface of the threaded portion of the body abuts against the cap. The rate of venting in this case is limited by the clearance between the cap and body surfaces.

Heat transfer during the fire exposure is modeled using COMSOL Multiphysics®, a finite element code. It is assumed that the rate of heat transfer is determined by the rate of thermal radiation and natural and forced convection to the B vial surfaces. Rates of heat transfer are computed for upright or recumbent vials, either engulfed by the fire or exposed to the fire over half the vial circumference.

The pressurization analysis is performed separately, using tabulated results from the heat transfer calculation. The pressurization analysis includes a correction to account for cooling of the oxide powder due to evaporation of the adsorbed moisture.

® COMSOL Multiphysics is a registered tradename of COMSOL, Inc., of Burlingame, Massachussets.

 This work was prepared under Federal Contract DE-AC09-08SR22470.

NOMENCLATURE

A, B, C	Antoine equation parameters
A_x	cross-sectional vent flow area, cm^2
c	sonic velocity at vent
C_L	loss coefficient for entrance flow at vent opening
c_{p,PuO_2}	specific heat for solid plutonium oxide
$c_{p,PuO_2,ev}$	contribution of moisture evaporation to the effective specific heat for the oxide
$c_{p,PuO_2,tot}$	total effective specific heat for the oxide with adsorbed moisture, including evaporation effects
C_R	compression factor for the o-ring, defined as the fractional compression of the o-ring from its uncompressed thickness to its final, seated thickness
d_h	hydraulic diameter for the vent passage
$E(H)$	modulus of elasticity for the o-ring material
f	Fanning friction factor for flow through the vent
f_{H_2O}	mass fraction of the plutonium oxide that is adsorbed moisture
H	Shore hardness for nitrile rubber
k	specific heat ratio for vent gas
L	length of the vent passage
M_1	Mach number for vent flow at entrance to vent
M_2	Mach number for vent flow at exit from vent
M_{H_2O}	molecular mass of water, 18 g/mol
m_{H_2O}	mass of adsorbed water
m_{PuO_2}	mass of plutonium dioxide in the vial
n_{H_2O}	number of moles of water adsorbed onto plutonium oxide
$n_{H_2O,ev}$	number of moles of water evaporated from the oxide
P	pressure
P_0	pressure inside the vial prior to the fire, assumed to be ambient pressure
P_a	ambient pressure
P_e	pressure inside the vial due to volumetric expansion
P_{H_2O}	pressure increase due to evaporation
ΔP_{leak}	minimum differential pressure for leaking across the o-ring
P_{max,H_2O}	maximum water vapor pressure if all adsorbed water evaporates
P_t	total pressure increase due to volumetric expansion and evaporation
$P_{t,adj}$	gauge pressure in B vial, adjusted for reduction in evaporation rate due to cooling
P_{v,H_2O}	water vapor pressure
$P_{v,H_2O,0}$	saturation water vapor pressure at temperature prior to fire exposure
$\left(\frac{dP}{dt}\right)_e$	rate of pressure increase due to volumetric expansion of gas inside the vial
Q	volumetric vent flow rate
R_g	ideal gas law constant
Re_c	Reynolds number for the vent flow, based on the sonic velocity
$\left(\frac{dT}{dt}\right)_{ox,adj}$	rate of temperature increase for oxide, adjusted for additional evaporation due to venting
$\left(\frac{dT}{dt}\right)_{ox}$	rate of temperature increase for oxide, from heat transfer analysis
T	temperature inside the vial at time t
t	duration of exposure to fumes from the fire
T_0	temperature inside the vial prior to the fire
T_{oring}	o-ring temperature
T_{oxide}	average oxide temperature
T_r	reference temperature, 273.15 K
V	interior volume of an empty vial
w_{gap}	width of the o-ring after compression at ambient temperature
w_{oring}	width of the o-ring prior to compression at ambient temperature
β_{nr}	coefficient of thermal expansion for nitrile rubber
ε	surface roughness
λ_{H_2O}	heat of vaporization for water
$\rho_{H_2O,v}$	water vapor density
ρ_{max,H_2O}	water vapor density from evaporation if all adsorbed moisture evaporates
ρ_{py,PuO_2}	pycnometric density of plutonium dioxide, 11.46 g/cm^3

B VIAL DESCRIPTION

The B vial has a diameter of 1.0 in. and a total height of 1.687 in. The B vial capacity is 8.38 cm^3. The B vial is constructed of 304L stainless steel. The B vial has a threaded cap. The threads are Unified Fine (UNF), 14 threads per in., with a nominal thread diameter of 0.875 in. The threaded height is 0.215 in. along the length of the B vial. The threads are sealed with a nitrile rubber o-ring that spans the gap between the cap and body. The o-ring is a Parker size 2-116-70, with an inner diameter of 0.737 in., a thickness of 0.103 in., and a Shore hardness rating of 70. Figure 1 shows a B vial, with the o-ring in place.

FIG 1. B VIAL

HEAT TRANSFER ANALYSIS

The temperature transients for the plutonium oxide and gas inside the B vial and the o-ring that seals this vial are calculated using Version 4.3 of COMSOL Multiphysics®. The finite element model assumes that the vial is heated by 1000 °C fumes from a fire on its circumference. An accurate geometric model of the vial consisting of the 304L stainless steel body, the nitrile rubber o-ring, and the plutonium oxide powder contents was constructed. Also included in the model is an air gap above the oxide layer. Figure 2 depicts the computational mesh for the model for the upright orientation; a similar mesh was constructed for the recumbent orientation.

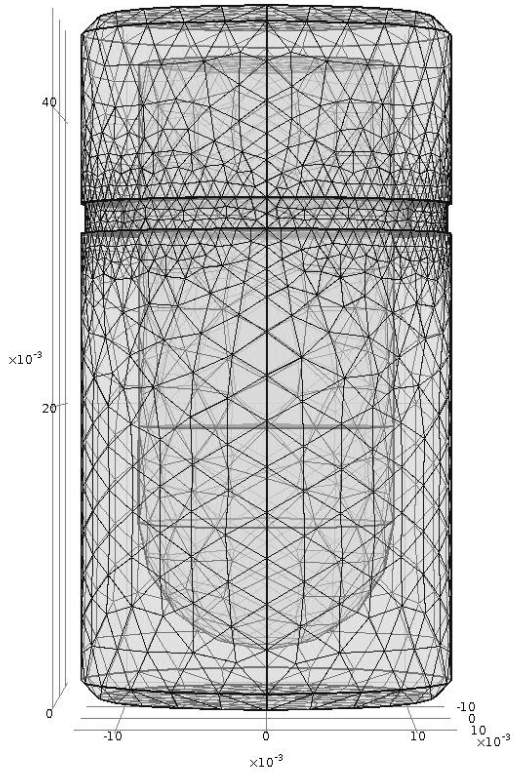

FIG 2. FINITE ELEMENT DISCRETIZATION FOR UPRIGHT B VIAL

The finite element simulation models heat conduction within the stainless steel body, the oxide, and the o-ring, and between their surfaces. The model accounts for heat transfer across the air gap inside the vial by thermal radiation only. Heat transfer from the fire fumes to the vial is modeled by including thermal radiation, convection, and conduction. The emissivity for the stainless steel surfaces is set conservatively at 0.9, which is a value typical for soot-covered surfaces. The o-ring emissivity is set at 0.94.[1] The heat transfer coefficient for the outside surfaces is evaluated using the Polhausen correlation for flow past a surface with a leading edge.[2] The thermal radiation boundary condition is applied to all surfaces of the recumbent vial and to all surfaces except the bottom surface of the upright vial, which is assumed to be insulated. The convective heat transfer model is applied only to the circumferential surfaces of both the upright and recumbent vials. The characteristic length for the heat transfer correlation is the height of the upright vial and the diameter of the recumbent vial. Exposure of one side of the vial to the fire is modeled by assuming that heat transfer over half of the circumference is to air at the initial ambient temperature. The top of the vertical vial and the end surfaces of the horizontal vial are assumed to be exposed to the fire, both for cases where the fire engulfs the entire vial surface and where only one side of the vial is exposed to the fire.

A detailed description of the estimation of the oxide powder thermal conductivity is provided, because the

heterogeneity of the powder complicates the evaluation of its equivalent conductivity , which is critical to the calculation of the oxide temperature and hence the vapor pressure of the adsorbed moisture. The properties of other materials are obtained primarily from tabulations of either default data built into COMSOL Multiphysics® or data from external sources. The properties of the 304 stainless steel vial body and air are provided by COMSOL Multiphysics®. The density and heat capacity of the nitrile rubber o-ring are specified as 1.0 g/cm^3 and 0.25 J/g/K,[3] and the o-ring thermal conductivity is set at 0.24 W/m/K.[4] The plutonium oxide density is specified as 2300 kg/m^3, based on typical measured bulk densities for plutonium oxide powders.

The thermal conductivity of the plutonium oxide powder is calculated using a LANL model that accounts for both conduction within and between the powder particles and thermal radiation between particles.[5]

The total effective heat capacity for the oxide is computed as the sum of the intrinsic plutonium oxide powder heat capacity and an equivalent heat capacity for evaporation of adsorbed moisture:

$$c_{p,PuO_2,tot} = c_{p,PuO_2} + c_{p,PuO_2,ev} \tag{1}$$

The intrinsic specific heat of plutonium dioxide without any adsorbed moisture, c_{p,PuO_2}, is based on a correlation that was developed as part of an Oak Ridge National Laboratory (ORNL) study of mixed oxide fuel properties.[6]

The equivalent heat capacity that corresponds to the latent heat required to evaporate adsorbed moisture up to its vapor pressure is given by

$$c_{p,PuO_2,ev} = \frac{\lambda_{H_2O}}{n_{H_2O}}\left(\frac{f_{H_2O}}{1-f_{H_2O}}\right)\frac{dn_{H_2O,ev}}{dT} \tag{2}$$

The following empirical expression is used to correlate the latent heat of water as a function of temperature at the moderate pressures present in the vial.[7]

$$\lambda_{H_2O} = 1000(3335 - 2.91T) \tag{3}$$

The number of moles of water evaporated from the oxide powder is given by

$$n_{H_2O,ev} = \frac{\min\left(P_{v,H_2O}, P_{max,H_2O}\right)V}{R_g T} \tag{4}$$

Substitution of this conditional expression into equation 2 yields, for $P_{v,H_2O} < P_{max,H_2O}$

$$c_{p,PuO_2,ev} = \frac{\lambda_{H_2O} V}{n_{H_2O} R_g}\left(\frac{f_{H_2O}}{1-f_{H_2O}}\right)\frac{d}{dT}\left(\frac{P_{v,H_2O}}{T}\right) \tag{5}$$

and, for $P_{v,H_2O} \geq P_{max,H_2O}$

$$c_{p,PuO_2,ev} = 0 \tag{6}$$

The total effective heat capacity is entered into the COMSOL Multiphysics® model as a tabulated function.

Venting reduces the rate of pressure increase in the vial not only directly but also by evaporative cooling of the oxide. It is assumed that the amount of gas exiting the vent is accompanied by an equal molar amount of gas evaporating from the oxide surface. Consequently, the rate of temperature increase for the oxide, on which the rate of evaporation is based, is reduced by the product of the venting rate for the vapor and the latent heat of vaporization, divided by the product of the oxide mass and the equivalent thermal conductivity of the oxide, according to the following expression

$$\left(\frac{dT}{dt}\right)_{ox,adj} = \left(\frac{dT}{dt}\right)_{ox} - \frac{\rho_{H_2O,v} k Q \lambda_{H_2O}}{m_{PuO_2} c_{p,PuO_2,tot}} \tag{7}$$

The rate of temperature increase for the oxide is adjusted for evaporative cooling in the pressurization analysis.

PRESSURIZATION ANALYSIS

The total pressure change during the fire transient is calculated by summing the contributions from volumetric expansion and evaporation of adsorbed moisture and subtracting the contribution from venting. Heating of noncondensable gas and moisture evaporation combine to give the total increase in the pressure.

$$P_t = P_e + P_{H_2O} \tag{8}$$

According to the ideal gas law, the rate of pressure increase due to volumetric expansion is related to the rate of temperature increase by

$$\left(\frac{dP}{dt}\right)_e = \frac{P_0}{T_0}\frac{dT}{dt} \tag{9}$$

The pressure due to volumetric expansion alone is obtained by integrating this expression to obtain

$$P_e = P_0 + \int_{t_0}^{t}\left(\frac{dP}{dt}\right)_e dt \tag{10}$$

It is assumed that the gas space inside the vial remains saturated with water vapor at all times, including at the start of the fire transient, until all adsorbed moisture evaporates. Therefore, the increase in the vapor pressure during the fire transient is given by

$$P_{H_2O} = \min\left(P_{v,H_2O} - P_{v,H_2O,0}, P_{max,H_2O}\right) \tag{19}$$

The maximum vapor pressure for evaporation of all water adsorbed on the plutonium dioxide is calculated as a function of the maximum vapor density in the vial using the ideal gas law:

$$P_{max,H_2O} = \frac{R_g T \rho_{max,H_2O}}{M_{H_2O}} \tag{20}$$

The maximum water vapor density is obtained by dividing the mass of adsorbed water by the free volume inside the vial:

$$\rho_{max,H_2O} = \frac{m_{H_2O}}{V - \dfrac{m_{PuO_2}}{\rho_{py,PuO_2}}} \tag{21}$$

The increase in the pressure due to evaporation of water is limited both by the vapor pressure and the amount of moisture adsorbed on the plutonium oxide inside the vial. The

approximate water vapor pressure is given by an Antoine equation of the form.[8]

$$P_{v,H_2O} = \left(\frac{14.696}{760}\right) 10^{\left(A - \frac{B}{T - T_r + C}\right)} \qquad (22)$$

The adjusted pressure increase due to venting is computed by applying implicit time differencing. The implicit differencing equation takes the form

$$P_{t,adj,j+1} = \left(\frac{P_{t,adj,j} + P_a + P_{t,j+1} - P_{t,j}}{1 + \left(t_{j+1} - t_j\right)\frac{kA_x M_0 c}{V}} \right) - P_a \qquad (23)$$

The second term in the denominator of equation 23 accounts for the effect of the vent flow. The flow term is multiplied by the heat capacity ratio to account for the pressure-volume work performed by the venting gases. The heat capacity ratio is estimated under the assumption that, because the principal component of the gas mixture in the vial at pressures significantly above atmospheric is water vapor, the venting is equivalent to adiabatic expansion of slightly superheated steam. The heat capacity ratio is assigned a value of 1.2, which is between the value of 1.135 for polytropic expansion of saturated (wet steam) and 1.3 for adiabatic expansion of superheated (dry) steam.[9]

The vent flow rate is evaluated using the isothermal compressible flow equation.[10]

$$\frac{4fL}{d_h} = \frac{1}{k}\left(\frac{1}{M_1^2} - \frac{1}{M_2^2}\right) + \ln\left(\frac{M_1^2}{M_2^2}\right) \qquad (24)$$

The term on the left side of equation 24 represents frictional losses in the vent flow channel. Entrance and exit losses are omitted, because these losses are negligible compared to the frictional losses in the long vent passage. Equation 24 is solved iteratively using Newton's method.

The friction losses are expressed as the product of the Fanning friction factor and the length of the flow path, divided by the hydraulic diameter of the flow channel. The friction factor is calculated as the sum of the laminar and turbulent factors, using the formula[11]

$$f = \frac{16}{Re_c M_1}\left(\frac{T_{oxide}}{T_{oring}}\right) + \left(\frac{1}{-4\log_{10}\left(\frac{\varepsilon}{3.7 d_h}\right)} \right)^2 \qquad (25)$$

The laminar friction factor coefficient of 16 for a round tube is assumed to be applicable for the actual flow geometry for the B vial vent; the decrease in the hydraulic diameter from that for a round tube at least partially accounts for the effect of the noncircular flow area. Von Karman's expression for turbulent flow in rough-walled channels is used to calculate the contribution of turbulence. The arithmetic addition of the laminar and turbulent friction factors implies that the total friction factor should be two times the laminar friction factor at the transition to turbulent flow; for the channel roughness factor for the vent flow. The friction factor is not reduced for flows on the laminar side of the turbulent transition, as would be the case for flow in a straight channel. This conservatism is an approximate way to account for the increase in the effective friction factor for the spiral flow through the gap in the screw threads. The relative surface roughness, $\frac{\varepsilon}{d_h}$, is arbitrarily set equal to 0.001.

An additional equation is needed to calculate the inlet pressure, P_1, as a function of the stagnation pressure, P_0. The following approximate expression has been used to relate the stagnation pressure to the inlet pressure and simultaneously account for flow entry losses.[12]

$$\frac{P_0}{P_1} = \left(1 + \left(\frac{3(k-1)}{4}\right) M_1^2\right)^{\frac{k}{k-1}} \qquad (26)$$

The loss coefficient acounts for a typical entrance loss of 0.5 velocity heads, which bounds the losses for both turbulent and laminar flow.

MODELING OF VENT PATHS

For venting of B vials with o-rings, the limiting vent path is assumed to follow the root of the threads between the body and cap of the vial. The threads are Unified Fine (UNF), 14 threads per in., with a nominal diameter of 0.875 in. along the threads. Standard thread design calls for rounded clearances between the troughs and the peaks of each thread. At the clearances, the peaks are truncated to flat surfaces, equal to 0.125 times the thread pitch at the outer thread peak and 0.250 times the thread pitch at the inner thread peak.[13] The troughs are rounded to provide a clearance opposite the truncated peaks. It is assumed that the rounded clearances take the shape of a circular chord section that spans a 120-degree arc, as shown by the hatched area in Figure 3. The analysis credits only the flow through the larger inner thread clearance, which has a hydraulic diameter of 168 μm.

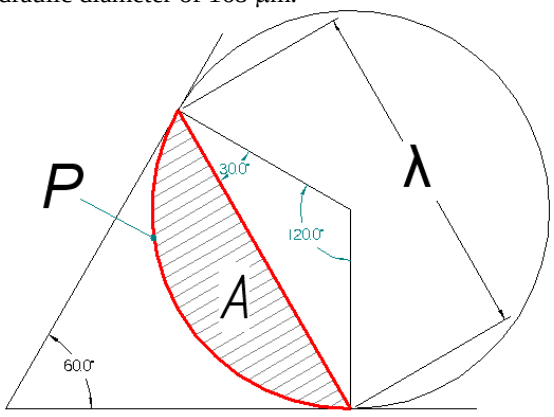

FIG 3. SCHEMATIC OF THREAD CLEARANCE GEOMETRY

The o-ring leak pressure is assumed to be the pressure at which the pressure differential across the o-ring equals the maximum contact pressure between the o-ring and its seating

surface. Maximum contact pressures for o-rings confined by various seating arrangements have been analyzed using finite element calculations.[14] For an o-ring seated between two parallel surfaces and unconstrained otherwise, the leak pressure is conservatively correlated as a function of the modulus of elasticity for the o-ring and the o-ring compression factor by

$$\Delta P_{leak} = \frac{14.696}{101325}\left(2.8383 C_R - 8.5051 {C_R}^2 + 18.6031 {C_R}^3\right) E(H) \quad (28)$$

The compression ratio is computed as the fractional difference between the o-ring thickness when not compressed and its thickness under compression. The calculation accounts for the additional compression that occurs as the o-ring undergoes thermal expansion during the fire transient. The equation for the compression ratio is

$$C_R = 1 - \frac{w_{gap}}{w_{oring}\left(1 + \beta_{nr}\left(T - T_0\right)\right)} \quad (29)$$

It is assumed that the o-ring is compressed from its original thickness of 0.103 in. to the recommended thickness of 0.082 in. at ambient temperature.[15] The thermal expansion coefficient for nitrile rubber is 6.2E-05 in./in./°F.[16]

The o-ring elasticity customarily is given in terms of the Shore hardness scale, which is related to the modulus of elasticity by the error function (erf) expression[16]

$$H = 100 \operatorname{erf}\left(0.0003186 E(H)^{0.5}\right) \quad (30)$$

The nominal Shore hardness for the B vial o-ring is 70, with an approximate upper bound of 77 that accounts for stiffening of the o-ring rubber with increasing temperature.[15] To bound the leak pressure, the hardness is set at 77 up to the point where the nitrile rubber in the o-ring begins to soften. The reduction in the hardness at higher temperatures is estimated based on the hardness versus temperature variation for fluorosilicone rubber, using information provided by Cupp's Industrial Supply, Inc., of Phoenix, Arizona.[17] The hardness of both nitrile rubber and fluorosilicone rubber is nearly constant at about 64.5 until just below 400 °F (approximately 200 °C), at which temperature the fluorosilicone rubber hardness rapidly decreases. For temperatures above 400 °F (388.47 K), a hardness correlation based on the Cupp information takes the form

$$H = \frac{77}{64.5} \max\left(64.5 - 6.9501\left(\frac{T(F) - 388.47}{100}\right)^2, 0\right) \quad (31)$$

Figure 4 shows the leak pressure derived from the preceding equations as a function of temperature.

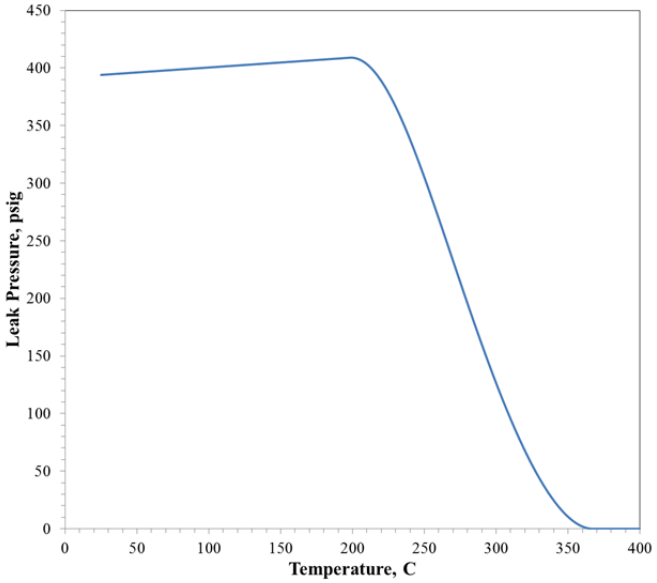

FIG 4. LEAK PRESSURES FOR THE B VIAL O-RING AS A FUNCTION OF TEMPERATURE

In the absence of an o-ring, the hydraulic diameter for contact between the vial body and cap is calculated for a representative diamond-shaped space between two saw tooth surfaces. Figure 5 depicts the geometry for the representative gap. In this figure, w is the gap between successive saw tooth ridges, θ is the angle of repose of a representative average ridge surface, and r_a is the average surface roughness, shown to be one quarter the peak-to-trough distance for the saw tooth.

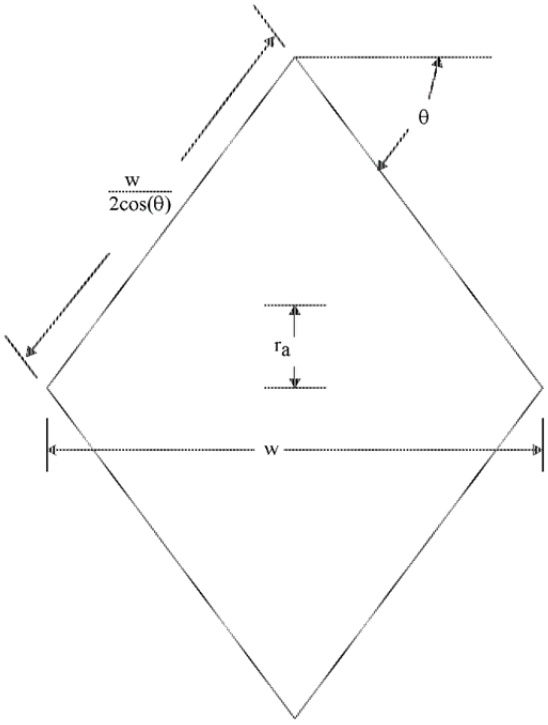

FIG 5. SCHEMATIC REPRESENTATION OF FLOW GAP BETWEEN TWO ROUGH SURFACES

INITIAL PRESSURIZATION PRIOR TO FIRE EXPOSURE

The effect of storage history is examined by analyzing pressure histories for oxide that is freshly packaged or aged oxide that has generated hydrogen gas due to radiolysis over a period of months or years. The vial pressure for fresh oxide is assumed to be equal to the ambient atmospheric pressure at the start of the fire exposure transient. The gauge pressure at the beginning of the transient for aged oxide is assumed to be equal to a maximum equilibrium pressure for long-term storage of plutonium oxide. This pressure is set at 82 psig, based on the results of hydrogen back pressure tests conducted by Duffey and Livingston.[18] The amount of adsorbed water is reduced by the amount of hydrogen generated on an equimolar basis. It is assumed that any oxygen generated by water radiolysis combines with the oxide and consequently is not released as a gas.

BENCHMARKING OF VENTING MODEL

The accuracy of the venting model for surface to surface contact is benchmarked using helium leak test data for a somewhat larger oxide storage vial, the so-called C vial. The C vial was not sealed with an o-ring. Consequently, the limiting vent path was through the gap where the top of the body seated against the cap. Five tests were conducted; results of the tests are shown in Figure 6.

The leak rate model was benchmarked by applying a multiplier to the estimated average gap thickness. To obtain a conservative estimate for the leak rate, the multiplier was set to match the slowest measured pressure decay rate, i.e., the decay rate for Test 3-2. A multiplier of 0.75 was used. As illustrated in Figure 6, this multiplier provided a close match between the measured and calculated pressure transient.

The C vial surfaces have a nominal roughness of 32 μin., compared to 63 μin. for the B vial surfaces. The B vial surface roughness in the model is set equal to the C vial value of 63 μin., so that the C vial benchmarking results do not require any scaling by a roughness factor. This simplification is conservative with respect to pressurization in that it results in a lower venting rate than would be predicted using the larger roughness. A sensitivity analysis is included to examine the effect of changes in the surface roughness on the maximum vial pressure. The sensitivity analysis compares pressure transients for equivalent surface roughnesses of 32, 48, and 64 μin.

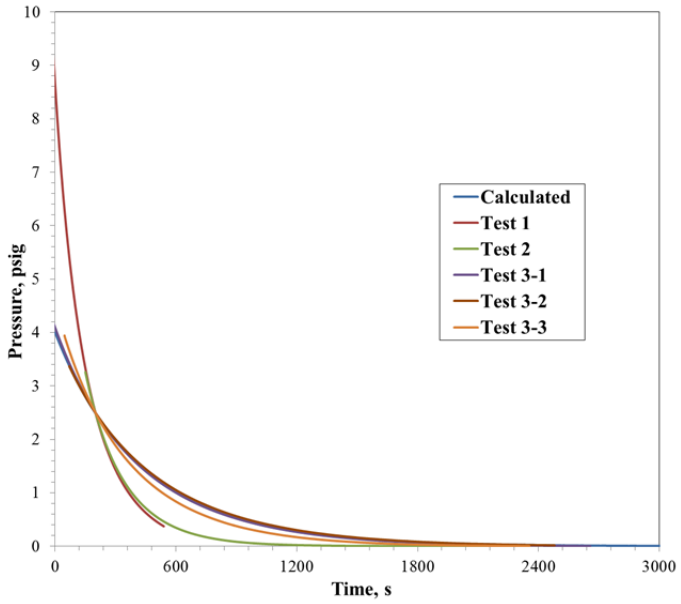

FIG 6. BENCHMARKING OF C VIAL HELIUM LEAK TESTS

DISCUSSION OF RESULTS

Figures 7 and 8 depict the results of the COMSOL Multiphysics® heat transfer analysis for upright and recumbent vials. Both temperature profiles are for a vial that is 1/3 filled with oxide containing 2 wt % moisture, after 100 seconds exposure to a 1000 °C fire on all sides. Note that the temperatures are displayed in degrees C. As these figures show, there are significant differences between the vial body and oxide temperatures and a significant temperature gradient within the oxide, due to the low thermal conductivity of the oxide. Because the o-ring has a lower thermal conductivity than the surrounding stainless steel, the maximum computed temperature was on the outside surface of the o-ring.

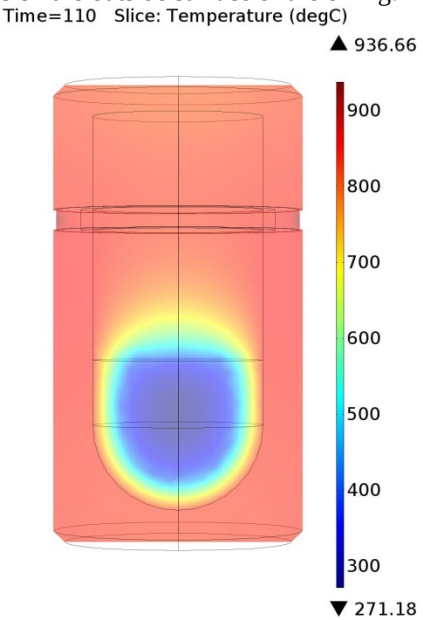

FIG 7. TYPICAL HEATING PROFILE IN AN UPRIGHT B VIAL

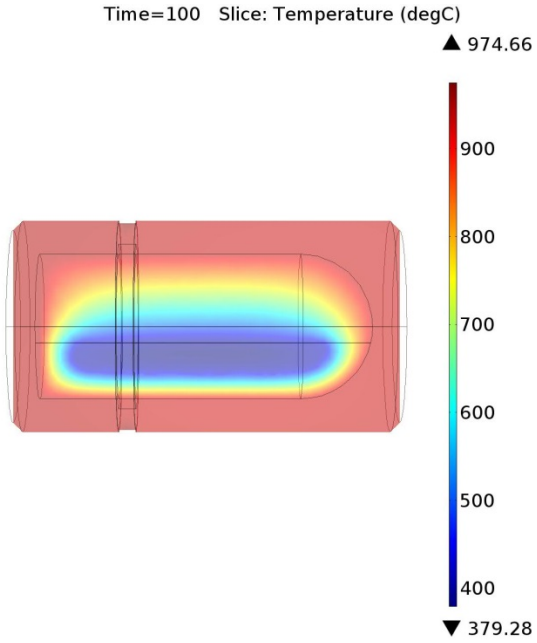

FIG 8. TYPICAL HEATING PROFILE IN A RECUMBENT B VIAL

Volume average temperatures for the oxide and gas inside the B vial and for the o-ring on the outside of the vial were computed from COMSOL Multiphysics® results for use in subsequent pressurization calculations. The o-ring temperature is needed to compute the release pressure for the o-ring. Figure 9 compares average gas, oxide, and o-ring temperatures for the same case as Figure 7 (an upright vial 1/3 filled with oxide containing 2 wt % moisture). It may be seen that the average gas temperatures is lower than the average o-ring temperature and that the average oxide temperature is significantly lower than the o-ring temperature.

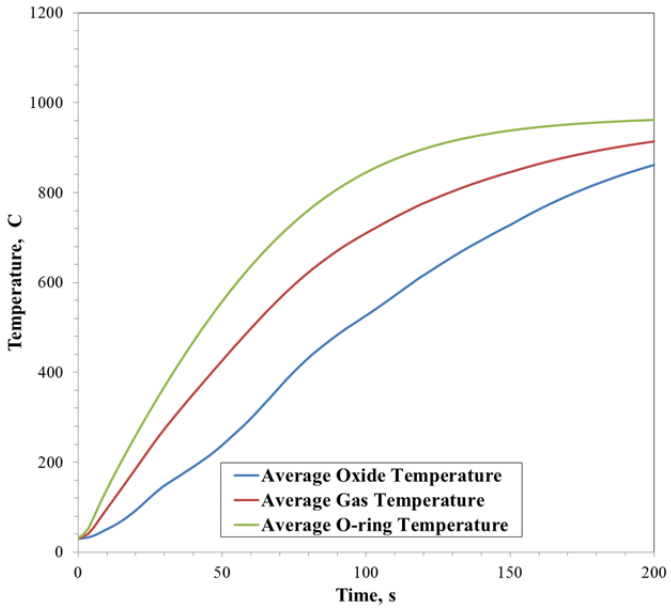

FIG 9. AVERAGE TEMPERATURES DURING EXPOSURE TO A 1000 °C FIRE OF AN UPRIGHT B VIAL

Figures 10 and 11 depict typical pressure transients inside the vial as functions of time and the average oxide temperature, for the same case as Figures 7 and 9. During the pressurization calculation, the oxide temperature shown in Figure 9 is adjusted for cooling due to evaporation of vented vapor. Separate transients are shown for no venting (a purely hypothetical case in which the o-ring does not lose its sealing properties), venting through the gap around the tips of the threads between the cap and the body, both with and without partial plugging by powder that is entrained into the vent channel, and venting through the gap between the top surface of the body and the cap if the cap is screwed onto the body until the top surface of the body is hand tight. The latter closure would occur in the absence of an o-ring.

As Figures 10 and 11 show, there are two transitions where the vial pressure exhibits a decrease in the rate of pressurization. The first transition, at an average oxide temperature of 131 °C, occurs when the vial becomes sufficiently pressurized and the o-ring heats to a point where the o-ring seal fails. The o-ring temperature at this point is 329 °C (see Figures 9 and 11). The second transition takes place when all of the moisture evaporates. (The initial moisture is computed from a moisture level of 2 wt % for an amount of plutonium oxide that fills the vial to 1/3 its capacity.)

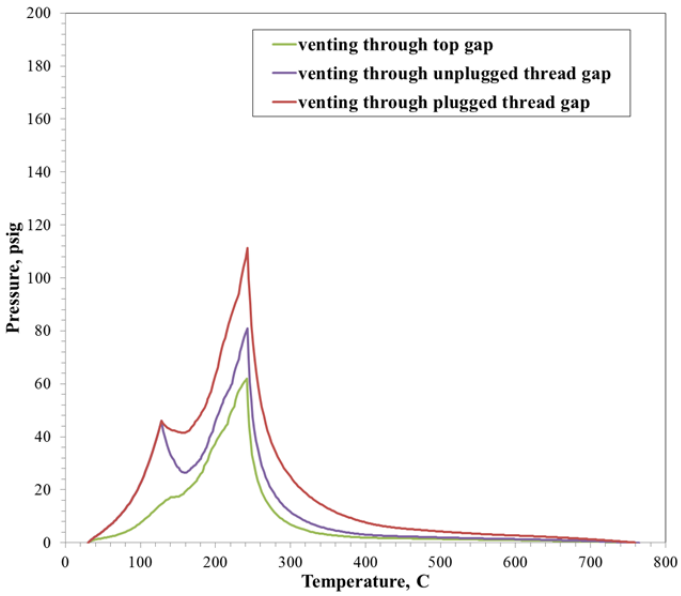

FIG 10. PRESSURE VARIATIONS FOR AN UPRIGHT B VIAL DURING EXPOSURE TO A 1000 °C FIRE, AS A FUNCTION OF AVERAGE OXIDE TEMPERATURE

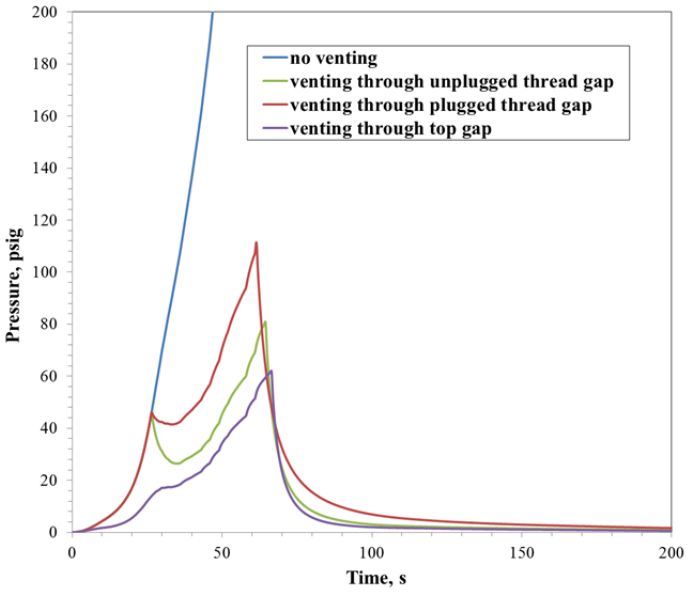

FIG 11. PRESSURE VARIATIONS FOR AN UPRIGHT B VIAL DURING EXPOSURE TO A 1000 °C FIRE, AS A FUNCTION OF TIME

The calculated pressures reached their highest levels when a recumbent B vial, engulfed by flames, vented through a partially obstructed thread path, after the o-ring seal failed. Figure 12 depicts the variation of the maximum pressure in psig with oxide moisture level and oxide fill fraction for this case, when the B vial is at ambient pressure prior to the fire. Figure 13 shows the same variations for this case, when the B vial is initially pressurized to 82 psig by radiolytic hydrogen generation. The maximum pressures during the fire transient are approximately equal with and without the initial hydrogen pressurization. With this initial pressurization, the maximum pressures are slightly higher for high oxide fill fractions and slightly lower for low oxide fill fractions. The decrease in the maximum pressure when the vial is initially pressurized occurs because more gas vents from the vial at low pressures before the pressurization reaches its maximum rate due to increased evaporation. An additional factor affecting this decrease is the reduction in the amount of moisture due to radiolysis. The maximum calculated pressure for any moisture level of 5 wt % or lower is 215 psig.

Table 1 lists maximum B vial pressures for venting through the gap between the cap and the body. The results in this table demonstrate that the surface roughness has a significant effect on venting rates and hence the maximum vial pressures.

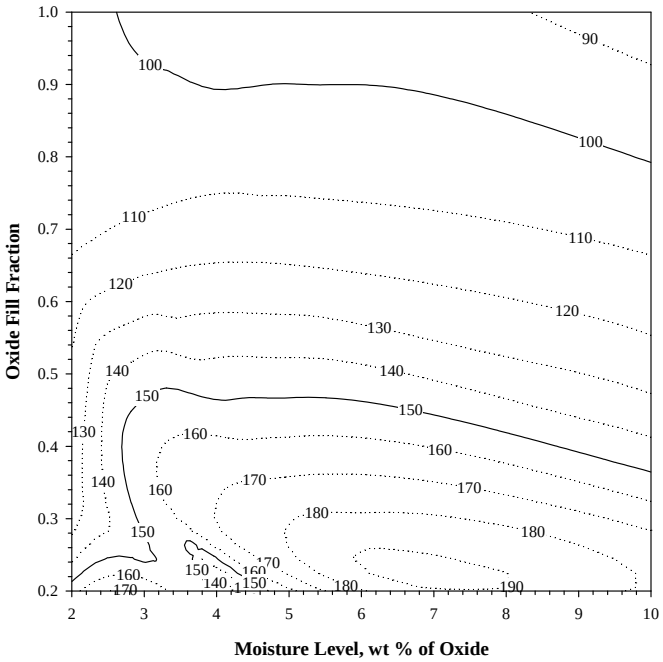

FIG 12. MAXIMUM VENTING PRESSURES IN PSIG FOR VENTING A RECUMBENT B VIAL THROUGH A PARTIALLY OBSTRUCTED THREAD

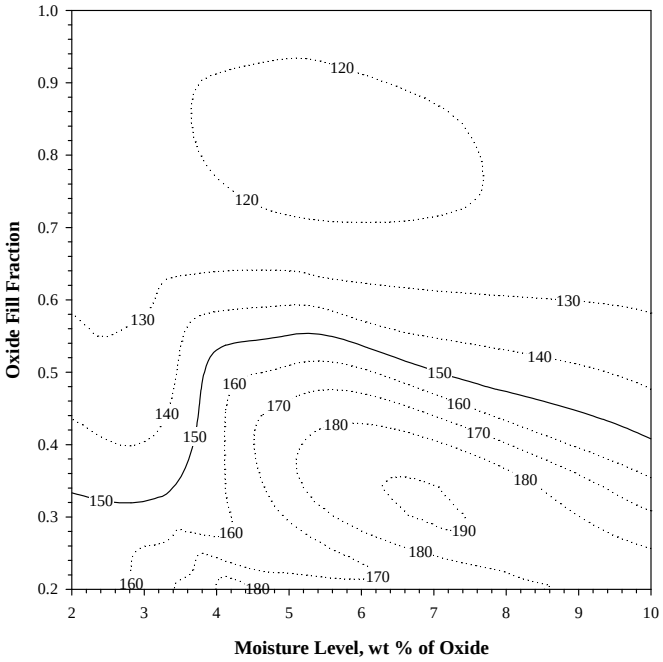

FIG 13. MAXIMUM VENTING PRESSURES IN PSIG FOR VENTING A RECUMBENT B VIAL THROUGH A PARTIALLY OBSTRUCTED THREAD, WITH INITIAL PRESSURIZATION BY RADIOLYTIC HYDROGEN

TABLE 1. MAXIMUM PRESSURES FOR VENTING OF A B VIAL THROUGH THE GAP BETWEEN THE CAP AND BODY FOR SURFACES OF VARYING ROUGHNESS

				Surface Roughness (μin.)		
B Vial	**Fire**	**Fill**	**H_2O**	**32**	**48**	**63**
Orientation	**Exp.**	**Fraction**	**(wt %)**	**Max. Pressure (psig)**		
Upright	Full	1/3 Full	2	190.3	102.4	62
Upright	Full	1/3 Full	3	238	124.1	75.2
Upright	Full	1/3 Full	5	298.8	139.7	76.9
Upright	Full	1/3 Full	10	305.1	131.1	71.8
Recumbent	Full	1/3 Full	2	218.2	109	67.6
Recumbent	Full	1/3 Full	3	261.4	132.2	78.1
Recumbent	Full	1/3 Full	5	316.7	144.6	79.7
Recumbent	Full	1/3 Full	10	316.9	135.6	74.2

SUMMARY AND CONCLUSIONS

A Los Alamos National Laboratory (LANL) study provides a reference point for bounding the maximum B vial pressures for the postulated fire exposure.(ref) This study indicates that the maximum moisture level that can be expected after calcining plutonium oxide at temperatures of at least 600 °C and ambient relative humidities no greater than 80% is approximately 4.4 wt %.[39] The maximum pressure for all cases analyzed at moisture levels of 5 wt % or less is 215 psig. This pressure is calculated for a recumbent vial filled to 1/10 capacity with oxide containing 5 wt % moisture, when that vial is engulfed by fire.

At each oxide fill ratio and moisture level, pressures are highest for the vent through the threads with blockage. The lowest maximum pressures are computed for flow through the clearance between the top surface of the vial and the cap, when this clearance is based on the nominal surface roughness of 63 μin.[8] The maximum pressure is relatively insensitive to the amount of adsorbed moisture and the amount of oxide in the vial. The calculated pressures for the upright vial are somewhat lower than the pressures for the recumbent vial, because the insulated bottom surface of the upright vial mitigates the rate of heating of the oxide and therefore lower the oxide temperature and water vapor pressure at the time the o-ring fails.

REFERENCES

1. "Emissivity Coefficients of Some Common Materials," The Engineering Toolbox, http://www.engineeringtoolbox.com/
2. Byrd, R. B., Stewart, W. E., and Lightfoot, E. N., Transport Phenomena, John Wiley & Sons, Inc., New York (1960), p. 410.
3. "Matbas: Nitrile Rubber," http://www.matbase.com/material/polymers/elastomers/nitrile-rubber/properties.
4. Lasance, C. J. M., "The Thermal Conductivity of Rubbers/Elastomers," Electronics Cooling, November, 2001, http://www.electronics-cooling.com/2001/11/the-thermal-conductivity-of-rubbers-elastomers.
5. Bielenberg, P. A., Prenger, F. C., Veirs, D. K., and Jones, G. F., "Effects of Pressure on Thermal Transport in Plutonium Oxide Powder," Int. J. Heat Mass Tran., 49, 3229-3239, 2006.
6. Carbajo, J. J., Yoder, G. L., Popov ,S. G., and Ivanov, V. K., "A Review of the Thermophysical Properties of MOX and UO_2 Fuels," J. Nucl. Mater., 299, 181-198, 2001.
7. Smith, A. W., "Heat of Evaporation of Water," Phys. Rev. (Series I), 25, 145-170, 1907.
8. Dortmund Data Bank Software and Separation Technology GmbH, www.ddbst.com.
9. Gebhardt, G. F., Steam Power Plant Engineering, John Wiley & Sons, Inc., New York (1917), p. 970.
10. Levenspiel, O., "The Discharge of Gases from a Reservoir through a Pipe," AIChE. J., 23(3), 402-403, 1977.
11. Green, D. W., ed., Perry's Chemical Engineers' Handbook, 6th ed., McGraw-Hill, New York (1984), p 5-24.
12. Zuk, J., Ludwig, L. P., and Johnson, R. L., "Quasi-One-Dimensional Compressible Flow across Face Seals and Narrow Slots," NASA Technical Note TN D-6668, Lewis Research Center, Cleveland, Ohio, May 1972.
13. Green, R. E., ed., Machinery's Handbook, 24th ed., Industrial Press, Inc., New York (1992).
14. Green, I. and English, C., "Stresses and Deformation of Elastomeric O-Ring Seals," 14th International Conference on Fluid Sealing, Firenze, Italy, April 6-8, 1994.
15. "Parker O-Ring Handbook", Parker Hannifin Corporation, Cleveland, Ohio (2007).
16. "Methods of Testing Vulcanized Rubber," British Standards 903, Part A7, British Standards Institution (1957).
17. "Physical Properties of O-Ring Compounds," Cupp 's Industrial Supply, Inc., http://cupps-industrial.com/oring/properties.html.
18. Duffey, J. M. and Livingston, R. M., "Gas Generation Testing of Plutonium Dioxide," Fifth Topical Meeting on Spent Nuclear Fuel and Fissile Materials Management, Charleston, South Carolina, September 17-20, 2002, WSRC-MS-2002-00705, September 17, 2002.